High-Temperature Thermal Stability of a Graphene Hall Effect Sensor on Defect-Engineered 4H-SiC(0001)

Tymoteusz Ciuk, Corinne Nouvellon, Fabien Monteverde, Beata Stańczyk, Krystyna Przyborowska, Dariusz Czołak, and Semir El-Ahmar, *Member, IEEE*

***Abstract*— In this letter, we demonstrate a Hall effect sensor in the technology of amorphous-Al_2O_3-passivated transfer-free p-type hydrogen-intercalated quasi-free-standing epitaxial Chemical Vapor Deposition graphene on semi-insulating high-purity on-axis 4H-SiC(0001), pre-epitaxially modified with 5-keV hydrogen (H^+) ions. The sensor operates between 305 K and 770 K, with a current-mode sensitivity of ∼75 V/AT and thermal stability below 0.15 %/K ($\leqslant$ 0.03 %/K in a narrower range between 305 K and 700 K). It is a promising two-dimensional platform for high-temperature magnetic diagnostics and plasma control systems for modern tokamak fusion reactors.**

***Index Terms*— Graphene, SiC, hall effect sensor.**

I. Introduction

MAGNETIC field sensors are gaining importance as novel applications emerge, including high-performance platforms [1]. Constant progress in nuclear fusion technologies dictates a road map for high-temperature (HT) magnetic diagnostics [2], [3] and sensors operating stably in a wide temperature range, from medium-high (473 K to 623 K) [4], [5], [6], up to the extreme (above 770 K) [7]. Changes in the toroidal magnetic field in industry-driven DEMO-class reactors are about to be monitored with Hall effect sensors operating at 473 K (ex-vessel position) and up to 773 K (in-vessel position). The current-mode sensitivity of HT devices strictly depends on the sensor active layer material. Below 673 K, AlGaN/GaN and InAlN/GaN heterostructures offer < 100 V/AT [6], [7], [8], compound-semiconductor thin films < 10 V/AT [4], [5], [9], metal and semimetal Hall sensors (Bi, Sb, Cr, Au, Mo, Ta, Cu) < 1 V/AT [10], [11]. The thermal stability of HT sensors is usually at the level of 0.1 %/K [4], [8], [9], [12].

Earlier, in [12], we reported on the application of hydrogen-intercalated quasi-free-standing (QFS) epitaxial Chemical Vapor Deposition (CVD) graphene on semi-insulating (SI) high-purity (HP) 4H-SiC(0001) in a Hall effect sensor verified between 300 K and 770 K. We reasoned that its performance followed the physics of a double-carrier system governed by holes in the QFS graphene and thermally-activated electrons in the SiC substrate. To restrict the evolution of the electron channel, we introduced the technology of pre-epitaxial modification of the 4H-SiC(0001) surface with hydrogen (H^+) (20 keV and 40 keV) and helium (He^+) (25 keV and 50 keV) ions to intentionally modify its post-epitaxial defect structure. Applying High-Resolution Photo-Induced Transient Spectroscopy, we identified 17 defect levels to prove that the protocol eliminates deep electron traps related to silicon vacancies in the charge state (2-/-) occupying the *h* and *k* sites of the 4H-SiC lattice, previously recognized as dominant in the process of thermal activation [13].

Of the two ions, the H^+ served the sensory platform better. Our final recommendation was to reduce the implantation energy to a sub-20-keV level in the hope that the sensitivity and hole mobility curves meet the optimum balance between the magnitude, linearity, and reproducibility. We reasoned that lowering the implantation energy would benefit the mobility curves, but only to the point that the pre-epitaxial modification brought an advantage.

In this communication, we demonstrate thermal stability and uniformity of hole concentration and mobility, sheet resistance, and sensitivity of an optimized Hall effect sensor in the technology of amorphous-Al_2O_3-passivated QFS epitaxial CVD graphene on SI HP 4H-SiC(0001), pre-epitaxially bombarded with 5-keV hydrogen (H^+) ions.

Manuscript received 20 June 2024; accepted 25 July 2024. Date of publication 31 July 2024; date of current version 27 September 2024. This work was supported in part by the National Science Centre, Poland, under Agreement OPUS 2019/33/B/ST3/02677; in part by the National Centre for Research and Development, Poland, under Agreement M-ERA.NET3/2021/83/I4BAGS/2022; in part by M-ERA.NET3 through European Union's Horizon 2020 Research and Innovation Programme under Agreement 958174; and in part by the Ministry of Education and Science, Poland, under Project 0512/SBAD/2420. The review of this letter was arranged by Editor D. Shahrjerdi. *(Corresponding author: Tymoteusz Ciuk.)*

Tymoteusz Ciuk, Beata Stańczyk, Krystyna Przyborowska, and Dariusz Czołak are with the Łukasiewicz Research Network–Institute of Microelectronics and Photonics, 02-668 Warsaw, Poland (e-mail: tymoteusz.ciuk@imif.lukasiewicz.gov.pl).

Corinne Nouvellon and Fabien Monteverde are with Materia Nova, 7000 Mons, Belgium.

Semir El-Ahmar is with the Institute of Physics, Poznan University of Technology, 61-138 Poznań, Poland (e-mail: semir.el-ahmar@put.poznan.pl).

Color versions of one or more figures in this letter are available at https://doi.org/10.1109/LED.2024.3436050.

Digital Object Identifier 10.1109/LED.2024.3436050

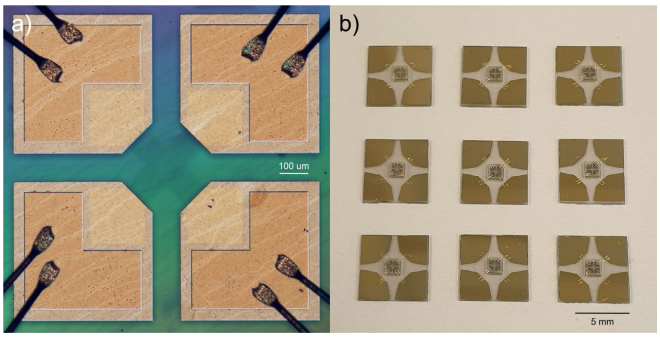

Fig. 1. (a) Top-view optical image of the individual sensor in the defect-engineered a-Al_2O_3/QFS-graphene/4H-SiC(0001) technology. (b) Photograph of mounted and wire-bonded sensors.

II. Fabrication and Methods

A. Graphene Epitaxy on Defect-Engineered 4H-SiC(0001)

The Hall effect sensor was produced in the graphene-on-SiC technology (GET® [14]). The graphene was transfer-free, p-type, *in-situ* hydrogen-intercalated [15], QFS, epitaxial CVD [16], [17], and statistically ~1.5-layer, within the understanding of the relative intensity of the SiC-related Raman-active A_1 mode at 964 cm^{-1} [18], [19]. It was grown at 1873 K in an Aixtron VP508 reactor on a 20-mm × 20-mm sample diced from a 4-in, 500-μm-thick, semi-insulating, high-purity, nominally on-axis 4H-SiC(0001) wafer (Wolfspeed Inc.), using thermally decomposed propane as the carbon-rich gas [20]. Before the epitaxy of graphene, the as-purchased 4H-SiC(0001) surface was implanted with a fixed dose of 1×10^{14} cm^{-2} of hydrogen (H^+) ions, with an energy of 5 keV, using an apparatus developed by Ionics SA. The expected penetration depth assessed with the Stopping and Range of Ions in Matter program (SRIM) was $d = 55$ nm.

B. Hall Effect Sensor Technology

The sample was processed into a batch of 96 *van der Pauw* structures [18]. Each structure was a 1.4-mm × 1.4-mm four-terminal device [12] featuring an oxygen-plasma-etched, equal-arm, cross-shaped [21] 100-μm × 300-μm graphene mesa, Ti/Au (10 nm/110 nm) current feed and voltage readout contacts, and a 100-nm-thick, atomic-layer-deposited, amorphous, non-stoichiometric [22] Al_2O_3 passivation [23] synthesized from trimethylaluminum and deionized water at 770 K in the Picosun R-200 Advanced reactor. The choice of this specific geometry, rather than of an optimized Hall bar, was justified by the authors' will to elucidate the transport properties of the 5-keV H^+-modified a-Al_2O_3/QFS-graphene/4H-SiC(0001) platform. The sample underwent dicing, and nine individual sensors were mounted onto and gold-wire-bonded to in-house-made 6.6-mm × 6.6-mm 364-μm-thick sapphire holders equipped with four Ti/Au (10 nm/190 nm) corner contacts. Fig. 1 (a) illustrates the optical photograph of an individual sensor, while Fig. 1 (b) mounted sensors.

C. Broad-Temperature Electrical Characterization

The sensors underwent verification under $I = 1$-mA direct current bias in an 0.556-T Ecopia AHT55T5 Hall effect measurement system in a broad temperature range (305 K to 770 K, with a step of 15 K) and exposure to ambient atmosphere. Their basic electrical properties, including hole concentration p_S, hole mobility μ_p, sheet resistance R_S, and current-mode sensitivity S_I (Hall coefficient), were measured and plotted as a function of temperature. The current-mode sensitivity followed Eq. 1:

$$S_I = \frac{dU_{Hall}}{dB}/I = 1/(p_S e)[V/AT] \tag{1}$$

where U_{Hall} is Hall voltage, B is magnetic field, I is feed current, p_S is hole concentration, and e is the unit charge.

To graphically visualize the thermal stability of the parameters, each measurement point was color-coded for its local change with temperature, according to Eq. 2:

$$\alpha_T = \left| \frac{\Delta P}{\Delta T}/P \right| \times 100\%[\%/K] \tag{2}$$

where P stands for either p_S, μ_p, R_S, or S_I, and T is the temperature. An absolute value of the normalized change was chosen, and the scale of α_T was equalized for all the transport parameters so that areas of corresponding stability could be easily detected.

III. Results and Discussion

The thermal stability scale was set between 0.0 %/K and 0.2 %/K for all the measured parameters. Its sign was purposefully ignored as the parameters may have opposite thermal tendencies.

Room-temperature (RT) verification (averaged over the 50000-μm^2 area of the cross-shaped QFS graphene mesa) revealed that the sensors exhibit p-type conductance with the hole density p_S at the level determined by the double polarization mechanism [22] of the SiC-related positive polarization [24], quantified by vector $P_0^{4H} = -2.0 \times 10^{-2}$ C/m^2 [25], and the negative effect of the a-Al_2O_3 passivation [22], fixing the p_S at approximately $+8 \times 10^{12}$ cm^{-2}. The p_S remains in agreement with the one measured in analogous materials and device technology but on non-modified 4H-SiC(0001) [12].

RT hole density was verified at ~8.0-8.7 × 10^{12} cm^{-2} ($p_{Smean} = 8.4 \times 10^{12}$ cm^{-2}, standard deviation $\sigma_p = 0.2 \times 10^{12}$ cm^{-2}). The p_S has a very stable character throughout the temperature range, with the α_T not exceeding 0.03 %/K at least up to ~700 K. Within the 700 - 770 K sub-range, α_T rises but does not exceed 0.15 %/K (Fig. 2).

RT hole mobility was confirmed at 1800 - 2000 cm^2/Vs ($\mu_{pmean} = 1860$ cm^2/Vs, $\sigma_\mu = 104$ cm^2/Vs). Its thermal stability throughout the temperature range is dynamic. Four conventional sub-ranges are detectable: ~300 K to ~400 K ($\alpha_T \leqslant 0.11$ %/K), ~400 K to ~600 K (α_T rises to 0.15 %/K), ~600 K to ~700 K (α_T reaches 0.2 %/K), and ~700 K to ~700 K (α_T drops to 0.15 %/K) (Fig. 3).

RT sheet resistance was measured at 350 - 450 Ω/sq ($R_{Smean} = 424$ Ω/sq, $\sigma_R = 56$ Ω/sq). The thermal stability of R_S is equally as dynamic as the stability of μ_p, with four detectable sub-ranges, in qualitative and quantitative agreement with the previous observation for μ_p (Fig. 4).

RT current-mode sensitivity was confirmed at 72 - 78 V/AT ($S_{Imean} = 74.4$ V/AT, $\sigma_S = 2.1$ V/AT). It follows the stable

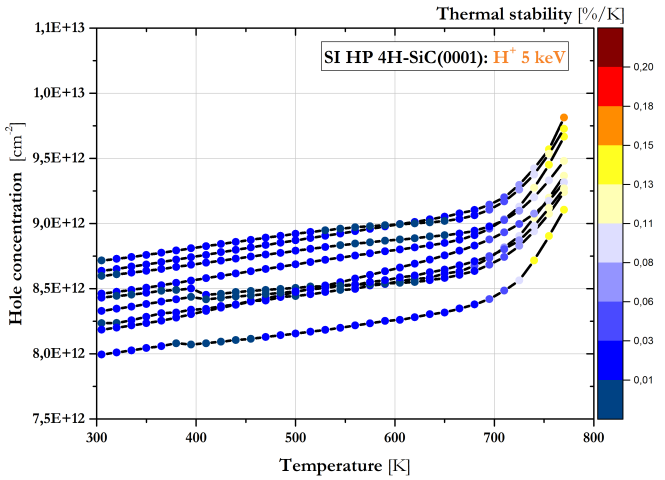

Fig. 2. Hole density profiles as a function of temperature (305 K to 770 K), measured in the nine Hall effect sensors presented in Fig. 1.

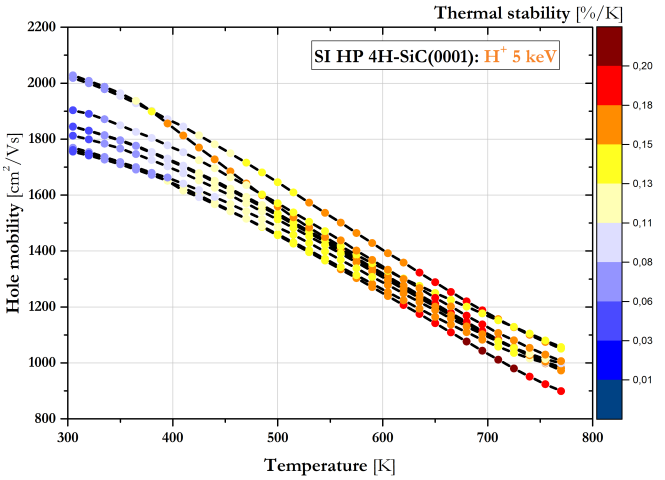

Fig. 3. Hole mobility profiles as a function of temperature (305 K to 770 K), measured in the nine Hall effect sensors presented in Fig. 1.

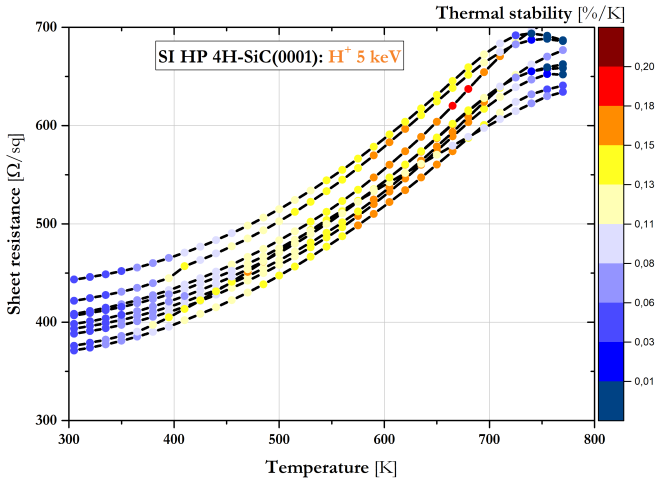

Fig. 4. Sheet resistance profiles as a function of temperature (305 K to 770 K), measured in the nine Hall effect sensors presented in Fig. 1.

character of p_S, with the α_T not exceeding 0.03 %/K at least up to ∼700 K ($S_{Imean} = 70.6$ V/AT, $\sigma_S = 1.8$ V/AT) and rising but not exceeding 0.15 %/K in the 700 - 770 K ($S_{Imean} = 66.1$ V/AT, $\sigma = 1.7$ V/AT) sub-range (Fig. 5). It is apparent that the undesirable contribution of the SiC-related electron

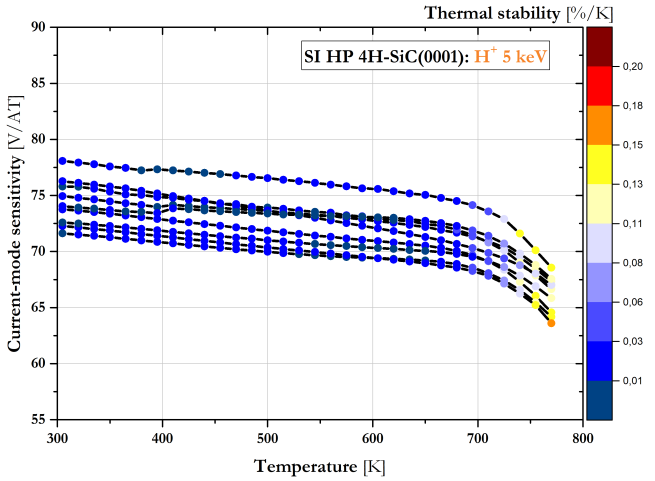

Fig. 5. Current-mode sensitivity as a function of temperature (305 K to 770 K), measured in the nine Hall effect sensors presented in Fig. 1.

channel to the double-carrier conductivity, is suppressed up to ∼700 K.

At 305 K, the thermal profiles display a percentile spread around their mean value ($\sigma/mean \times 100\%$) of p_S (2.8 %), μ_p (5.6 %), R_S (13.2 %), and S_I (2.8 %). At 770 K, the dispersion is down to p_S (2.6 %), μ_p (4.7 %), R_S (10.4 %), and S_I (2.6 %). This low variation is possible only because direct epitaxial growth does not require a polymer-assisted transfer [26]; it is elementally pure and void of substitutional dopants, and its charge carrier type and density are determined solely by the SiC-related vector of spontaneous polarization. The vestigial dispersion is traced to the developed topography of epitaxial graphene, marked with a fingerprint-like combination of micrometer-scale terraces and nanometer-scale steps [19], [27]. It remains an inherent feature of this technology and the primary source of offset voltage (here, at 305 K: from ∼6 mV to ∼83 mV, with one sensor exhibiting ∼224 mV, and at 770 K: from ∼10 mV to ∼121 mV, with the one sensor proving ∼366 mV).

IV. Conclusion

The Hall effect sensor fabricated in the technology of amorphous-Al_2O_3-passivated QFS epitaxial CVD graphene on defect-engineered semi-insulating high-purity nominally on-axis 4H-SiC(0001), pre-epitaxially implanted with 5-keV hydrogen (H^+) ions, operates between 305 K and 770 K and offers current-mode sensitivity of ∼75 V/AT. Throughout this temperature range, its hole mobility and sheet resistance maintain thermal stability $\alpha_T \leqslant 0.2$ %/K, while its hole density and current-mode sensitivity $\alpha_T \leqslant 0.15$ %/K. In a narrower range, between 305 K and 700 K, the stability of the current-mode sensitivity $\alpha_T \leqslant 0.03$ %/K. The sensor is a promising two-dimensional platform for high-temperature magnetic diagnostics and plasma control systems for modern tokamak fusion reactors.

References

[1] B. T. Schaefer, L. Wang, A. Jarjour, K. Watanabe, T. Taniguchi, P. L. McEuen, and K. C. Nowack, "Magnetic field detection limits for ultraclean graphene Hall sensors," *Nature Commun.*, vol. 11, no. 1, pp. 1–8, Aug. 2020, doi: 10.1038/s41467-020-18007-5.

[2] W. Biel, R. Albanese, R. Ambrosino, M. Ariola, M. V. Berkel, I. Bolshakova, K. J. Brunner, R. Cavazzana, M. Cecconello, S. Conroy, A. Dinklage, I. Duran, R. Dux, T. Eade, S. Entler, G. Ericsson, E. Fable, D. Farina, L. Figini, C. Finotti, T. Franke, L. Giacomelli, L. Giannone, W. Gonzalez, A. Hjalmarsson, M. Hron, F. Janky, A. Kallenbach, J. Kogoj, R. König, O. Kudlacek, R. Luis, A. Malaquias, O. Marchuk, G. Marchiori, M. Mattei, F. Maviglia, G. De Masi, D. Mazon, H. Meister, K. Meyer, D. Micheletti, S. Nowak, C. Piron, A. Pironti, N. Rispoli, V. Rohde, G. Sergienko, S. El Shawish, M. Siccinio, A. Silva, F. da Silva, C. Sozzi, M. Tardocchi, M. Tokar, W. Treutterer, and H. Zohm, "Diagnostics for plasma control–from ITER to DEMO," *Fusion Eng. Design*, vol. 146, pp. 465–472, Sep. 2019, doi: 10.1016/j.fusengdes.2018.12.092.

[3] S. El-Ahmar, M. J. Szary, T. Ciuk, R. Prokopowicz, A. Dobrowolski, J. Jagiełło, and M. Ziemba, "Graphene on SiC as a promising platform for magnetic field detection under neutron irradiation," *Appl. Surf. Sci.*, vol. 590, Jul. 2022, Art. no. 152992, doi: 10.1016/j.apsusc.2022.152992.

[4] S. El-Ahmar, J. Jankowski, P. Czaja, W. Reddig, M. Przychodnia, J. Raczyński, and W. Koczorowski, "Magnetic field sensor operating from cryogenics to elevated temperatures," *IEEE Sensors Lett.*, vol. 7, no. 8, pp. 1–4, Aug. 2023, doi: 10.1109/LSENS.2023.3294525.

[5] W. Reddig, M. Przychodnia, T. Ciuk, and S. El-Ahmar, "High-temperature stability of sensor platforms designed to detect magnetic fields in a harmful radiation environment," *IEEE Sensors Lett.*, vol. 7, no. 8, pp. 1–4, Aug. 2023, doi: 10.1109/LSENS.2023.3297795.

[6] K. M. Dowling, H. S. Alpert, A. S. Yalamarthy, P. F. Satterthwaite, S. Kumar, H. Köck, U. Ausserlechner, and D. G. Senesky, "Micro-tesla offset in thermally stable AlGaN/GaN 2DEG Hall plates using current spinning," *IEEE Sensors Lett.*, vol. 3, no. 3, pp. 1–4, Mar. 2019, doi: 10.1109/LSENS.2019.2898157.

[7] H. S. Alpert, C. A. Chapin, K. M. Dowling, S. R. Benbrook, H. Köck, U. Ausserlechner, and D. G. Senesky, "Sensitivity of 2DEG-based Hall-effect sensors at high temperatures," *Rev. Sci. Instrum.*, vol. 91, no. 2, Feb. 2020, Art. no. 025003, doi: 10.1063/1.5139911.

[8] S. Koide, H. Takahashi, A. Abderrahmane, I. Shibasaki, and A. Sandhu, "High temperature Hall sensors using AlGaN/GaN HEMT structures," *J. Phys., Conf. Ser.*, vol. 352, Mar. 2012, Art. no. 012009, doi: 10.1088/1742-6596/352/1/012009.

[9] J. Jankowski, S. El-Ahmar, and M. Oszwaldowski, "Hall sensors for extreme temperatures," *Sensors*, vol. 11, no. 1, pp. 876–885, Jan. 2011, doi: 10.3390/s110100876.

[10] S. El-Ahmar, M. Przychodnia, J. Jankowski, R. Prokopowicz, M. Ziemba, M. J. Szary, W. Reddig, J. Jagiełło, A. Dobrowolski, and T. Ciuk, "The comparison of InSb-based thin films and graphene on SiC for magnetic diagnostics (don't short) under extreme conditions," *Sensors*, vol. 22, no. 14, p. 5258, Jul. 2022, doi: 10.3390/s22145258.

[11] S. Entler, Z. Soban, I. Duran, K. Kovarik, K. Vyborny, J. Sebek, S. Tazlaru, J. Strelecek, and P. Sladek, "Ceramic-chromium Hall sensors for environments with high temperatures and neutron radiation," *Sensors*, vol. 21, no. 3, p. 721, Jan. 2021, doi: 10.3390/s21030721.

[12] T. Ciuk, B. Stanczyk, K. Przyborowska, D. Czolak, A. Dobrowolski, J. Jagiello, W. Kaszub, M. Kozubal, R. Kozlowski, and P. Kaminski, "High-temperature Hall effect sensor based on epitaxial graphene on high-purity semiinsulating 4H-SiC," *IEEE Trans. Electron Devices*, vol. 66, no. 7, pp. 3134–3138, Jul. 2019, doi: 10.1109/TED.2019.2915632.

[13] T. Ciuk, R. Kozłowski, A. Romanowska, A. Zagojski, K. Piętak-Jurczak, B. Stańczyk, K. Przyborowska, D. Czołak, and P. Kamiński, "Defect-engineered graphene-on-silicon-carbide platform for magnetic field sensing at greatly elevated temperatures," *Carbon Trends*, vol. 13, Dec. 2023, Art. no. 100303, doi: 10.1016/j.cartre.2023.100303.

[14] Lukasiewicz Research Network Institute of Microelectronics and Photonics. (2024). *Graphene Epitaxy Technologies*. [Online]. Available: http://www.graphene2get.com

[15] M. J. Szary, S. El-Ahmar, and T. Ciuk, "The impact of partial h intercalation on the quasi-free-standing properties of graphene on SiC(0001)," *Appl. Surf. Sci.*, vol. 541, Mar. 2021, Art. no. 148668, doi: 10.1016/j.apsusc.2020.148668.

[16] T. Ciuk and W. Strupinski, "Statistics of epitaxial graphene for Hall effect sensors," *Carbon*, vol. 93, pp. 1042–1049, Nov. 2015, doi: 10.1016/j.carbon.2015.06.032.

[17] T. Ciuk, P. Caban, and W. Strupinski, "Charge carrier concentration and offset voltage in quasi-free-standing monolayer chemical vapor deposition graphene on SiC," *Carbon*, vol. 101, pp. 431–438, May 2016, doi: 10.1016/j.carbon.2016.01.093.

[18] A. Dobrowolski, J. Jagiełło, D. Czołak, and T. Ciuk, "Determining the number of graphene layers based on Raman response of the SiC substrate," *Phys. E, Low-Dimensional Syst. Nanostruct.*, vol. 134, Oct. 2021, Art. no. 114853, doi: 10.1016/j.physe.2021.114853.

[19] A. Dobrowolski, J. Jagiełło, K. Piętak-Jurczak, M. Wzorek, D. Czołak, and T. Ciuk, "Spectroscopic properties of close-to-perfect-monolayer quasi-free-standing epitaxial graphene on 6H SiC(0001)," *Appl. Surf. Sci.*, vol. 642, Jan. 2024, Art. no. 158617, doi: 10.1016/j.apsusc.2023.158617.

[20] W. Strupinski, K. Grodecki, A. Wysmolek, R. Stepniewski, T. Szkopek, P. E. Gaskell, A. Grüneis, D. Haberer, R. Bozek, J. Krupka, and J. M. Baranowski, "Graphene epitaxy by chemical vapor deposition on SiC," *Nano Lett.*, vol. 11, no. 4, pp. 1786–1791, Apr. 2011, doi: 10.1021/nl200390e.

[21] T. Ciuk, O. Petruk, A. Kowalik, I. Jozwik, A. Rychter, J. Szmidt, and W. Strupinski, "Low-noise epitaxial graphene on SiC Hall effect element for commercial applications," *Appl. Phys. Lett.*, vol. 108, no. 22, pp. 1–6, May 2016, doi: 10.1063/1.4953258.

[22] K. Piętak-Jurczak, J. Gaca, A. Dobrowolski, J. Jagiełło, M. Wzorek, A. Zalewska, and T. Ciuk, "Origin of the double polarization mechanism in aluminum-oxide-passivated quasi-free-standing epitaxial graphene on 6H-SiC(0001)," *ACS Appl. Electron. Mater.*, vol. 6, no. 3, pp. 1729–1739, Mar. 2024, doi: 10.1021/acsaelm.3c01627.

[23] K. Piętak, J. Jagiełło, A. Dobrowolski, R. Budzich, A. Wysmołek, and T. Ciuk, "Enhancement of graphene-related and substrate-related Raman modes through dielectric layer deposition," *Appl. Phys. Lett.*, vol. 120, no. 6, Feb. 2022, Art. no. 063105, doi: 10.1063/5.0082694.

[24] J. Ristein, S. Mammadov, and T. Seyller, "Origin of doping in quasi-free-standing graphene on silicon carbide," *Phys. Rev. Lett.*, vol. 108, no. 24, Jun. 2012, Art. no. 246104, doi: 10.1103/physrevlett.108.246104.

[25] J. Sławińska, H. Aramberri, M. C. Muñoz, and J. I. Cerdá, "Ab initio study of the relationship between spontaneous polarization and p-type doping in quasi-freestanding graphene on H-passivated SiC surfaces," *Carbon*, vol. 93, pp. 88–104, Nov. 2015, doi: 10.1016/j.carbon.2015.05.025.

[26] A. Dobrowolski, J. Jagiełło, T. Ciuk, K. Piętak, and E. B. Możdżyńska, "Layer-resolved Raman imaging and analysis of parasitic ad-layers in transferred graphene," *Appl. Surf. Sci.*, vol. 608, Jan. 2023, Art. no. 155054, doi: 10.1016/j.apsusc.2022.155054.

[27] T. Ciuk, S. Cakmakyapan, E. Ozbay, P. Caban, K. Grodecki, A. Krajewska, I. Pasternak, J. Szmidt, and W. Strupinski, "Step-edge-induced resistance anisotropy in quasi-free-standing bilayer chemical vapor deposition graphene on SiC," *J. Appl. Phys.*, vol. 116, no. 12, Sep. 2014, Art. no. 123708, doi: 10.1063/1.4896581.